ChemPhysChem

Supporting Information

Electrochemical and Thermal Evolution of P2 $Na_{2/3}MnO_2$

B. D. K. K. Thilakarathna,* Uttam Mittal, Jian Peng, Daniel Brocklebank, Helen E. A. Brand, and Neeraj Sharma*

Electrochemical and Thermal Evolution of P2 $Na_{2/3}MnO_2$

B. D. K. K. Thilakarathna*[a], Uttam Mittal[a], Jian Peng[a], Daniel Brocklebank[a], Helen E. A. Brand[b], Neeraj Sharma[a]

[a] *School of Chemistry, UNSW Sydney NSW 2052, Australia*

[b] *Australian Synchrotron, Australian Nuclear Science and Technology Organisation, 800 Blackburn Road, Clayton, Victoria 3168, Australia.*

Corresponding author: b.thilakarathna@unsw.edu.au

SUPPORTING INFORMATION

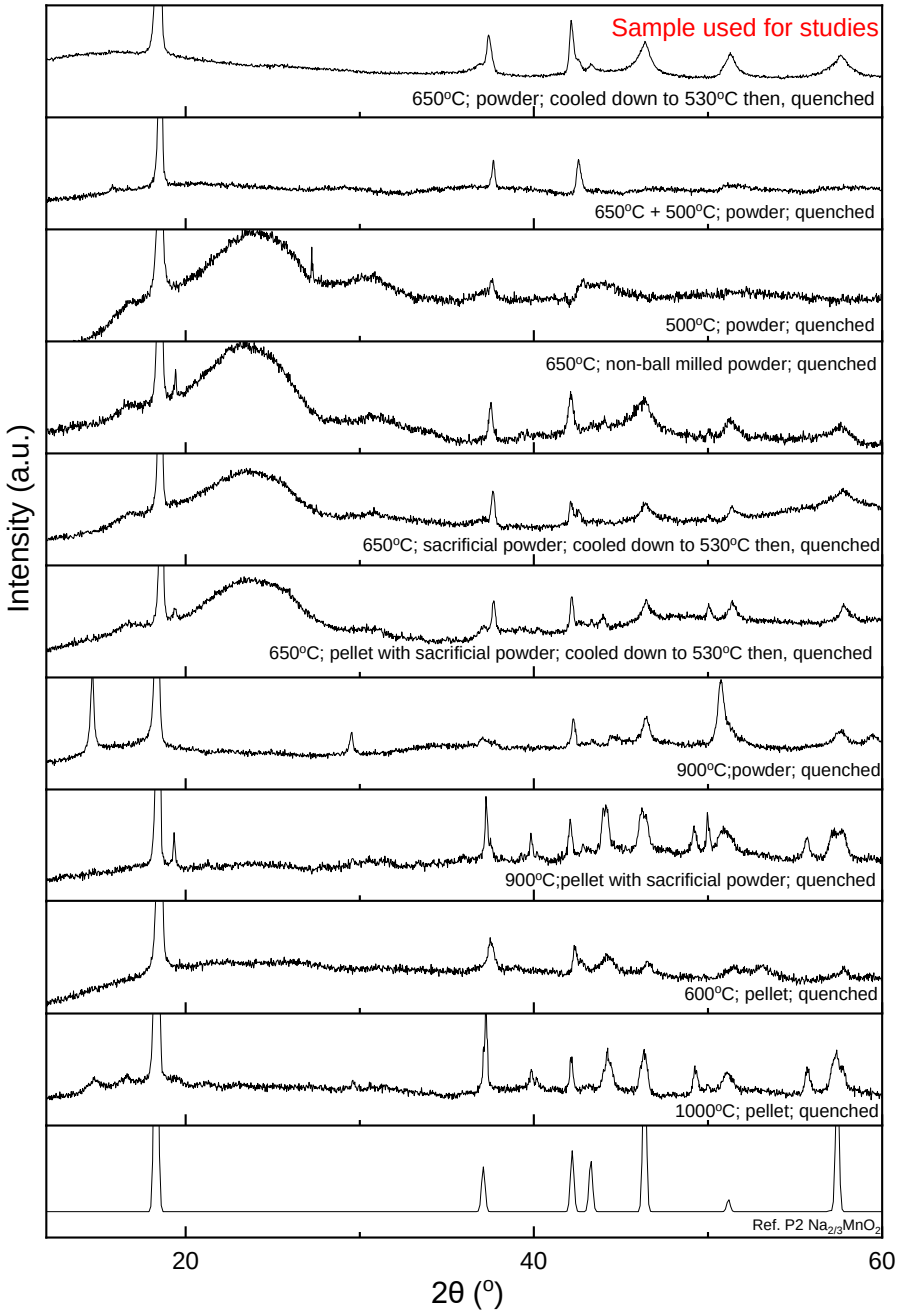

Figure S1: Diffraction data (λ = 1.7902 Å), of optimization of the synthesis procedure for P2 $Na_{2/3}MnO_2$, the reference pattern is from [29] ICSD no. 01-087-4156, *a* = 2.869 and *c* = 11.248 Å adopting *P6₃/mmc* space group symmetry. The sample used for this work is shown on the top panel, that is synthesized at 650°C cooled to 530°C and quenched.

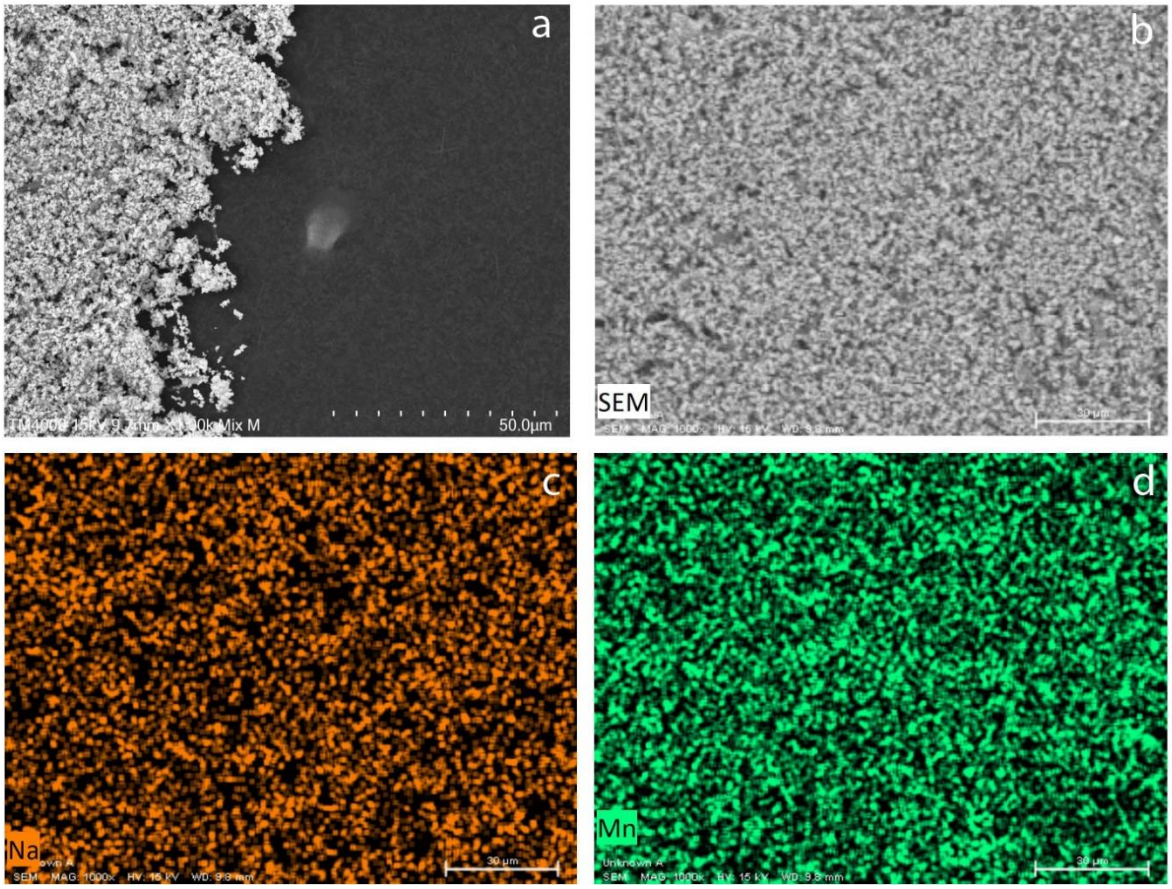

Figure S2: SEM images a) and b) of the synthesized P2 $Na_{2/3}MnO_2$ at x1000 magnification, EDS mapping of c) Na and d) Mn elements.

Table S1: Ratios determined from EDS analysis.

Test	Na	Mn	Na/Mn
1	3.7(5)	6.2(9)	0.60(11)
2	15(1)	19(1)	0.76(17)
3	9.2(8)	14(1)	0.68(9)
Avg.			0.68(5)

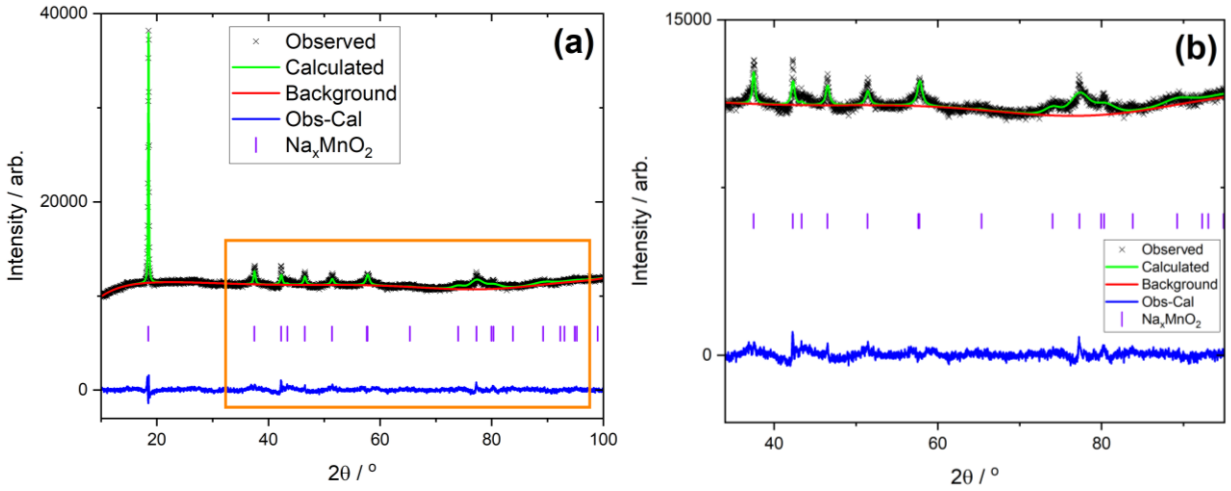

Figure S3: (a) Rietveld-refined fit (λ = 1.7902 Å) of the P2 Na_xMnO_2 powder at room temperature and (b) shows a zoom between 34 < 2θ < 95°, the region indicated by the box in (a).

Table S2: Crystallographic parameters for $Na_{2/3}MnO_2$ at RT refined against X-ray powder diffraction data. For this refinement, the lattice parameters, background, scale, zero offset, preferred orientation (spherical harmonics), profile and size/microstrain terms were refined initially. These were fixed and only the lattice parameters and atomic parameters were refined in the final stages. This approach was used as significant preferred orientation was observed and changes in peak shape were noted as a function of 2θ.

Space group: P6₃/mmc, *a* = 2.864(1) Å, *c* = 11.1390(3) Å, V = 79.16(3) Å^3.

Atom	Site	*x*	*y*	*z*	$U_{iso} \times 100$	*Occupancy*
Na1	*2b*	0.0000	0.0000	0.2500	1.0(7)	0.35
Na2	*2c*	0.3333	0.6667	0.7500	3.2(9)	0.35
Mn	*2a*	0.0000	0.0000	1.0000	3.5(2)	1.0
O	*4f*	0.3333	0.6667	0.0877(6)	0.1(3)	1.0

With no changes to the atomic parameters from ref. 29 χ^2 =3.1, R_{wp}=1.65%
With 8 variables after the approach described above χ^2 =2.4, R_{wp}=1.45%

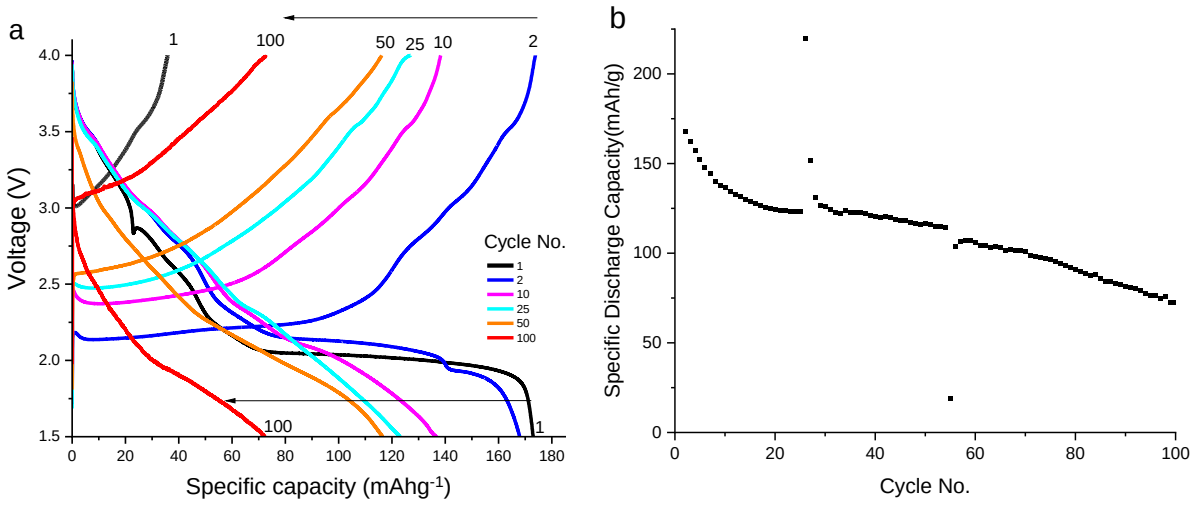

Figure S4: a) The voltage vs. specific charge/discharge capacity of P2 $Na_{2/3}MnO_2$ at selected cycles. b) Specific discharge capacity as a function of cycle number.

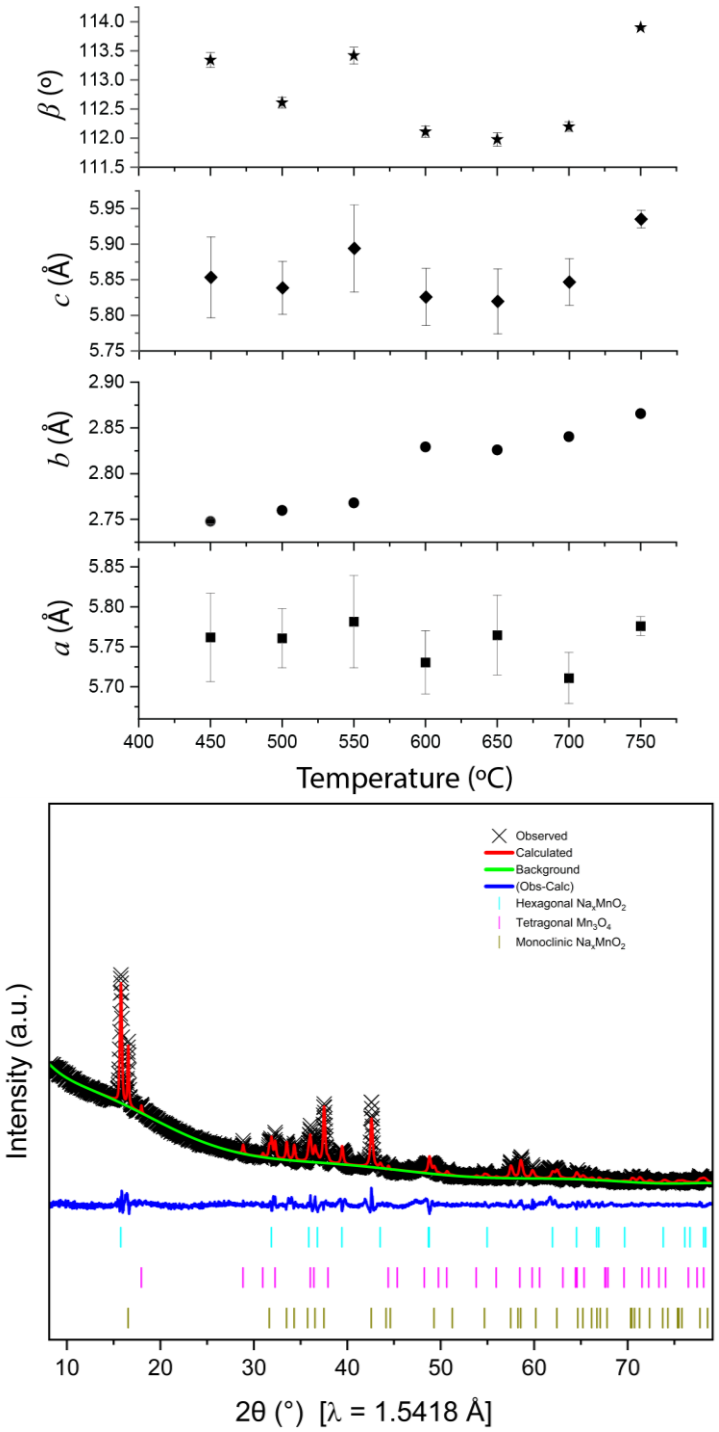

Figure S5. (a) Lattice parameter evolution of monoclinic phase during the thermal treatment of P2 $Na_{2/3}MnO_2$ under N_2 environment. (b) Rietveld-refined fit of structural models to the room temperature (post heat-treatment) sample.

Table S3: Lattice parameters of reported Na_xMnO_2 phases where 0.5<x<0.8.

Crystal system	**Sodium content (x)**	***a* (Å)**	***b* (Å)**	***c* (Å)**	**Vol. (Å^3)**	**Space group**	**Ref.**
Hexagonal	0.272	2.8763(3)	2.8763(3)	11.2404(17)	80.53	*P6$_3$/mmc*	14
Orthorhombic	0.39	9.1025(8)	26.340(2)	2.8300(2)	678.52	*Pbam*	45
Orthorhombic	0.319	9.0966(8)	26.357(2)	2.8242(2)	677.13	*Pbam*	14
Hexagonal	0.437	2.8749(2)	2.8749(2)	11.1400(5)	79.74	*P6$_3$/mmc*	14
Hexagonal	0.7	2.8911(4)	2.8911(4)	11.109(1)	80.41	*P6$_3$/mmc*	14
		2.8882(3)	2.8882(3)	11.1987(17)	80.9		
		2.88067(18)	2.88067(18)	11.1312(4)	80.00		
		2.8727(5)	2.8727(5)	11.2499(8)	80.40		
Orthorhombic	0.7	2.7937(2)	5.5896(3)	11.4116(1)	178.20	*Cmca*	23
		2.7980(1)	5.4400(3)	11.4079(2)	173.64		
Hexagonal	0.67	2.86204	2.86204	11.20364	79.47	*P6$_3$/mmc*	46
Hexagonal	0.66	2.869	2.869	11.248	80.18	*P6$_3$/mmc*	29
Orthorhombic	0.66	2.873	5.08	11.265	164.41	*Cmcm*	29
Orthorhombic	0.491	9.092	26.4754	2.8259	680.23	*Pbam*	47
Hexagonal	0.478	2.8869(4)	2.8869(4)	11.1886(8)	80.76	*P6$_3$/mmc*	14
Orthorhombic	1	2.859	6.338	4.785	*86.71*	*Pmnm*	48
Monoclinic (β=113.1^o)	1	5.662	2.86	5.799	86.38	*C2/m*	49
Orthorhombic	1	2.8477(2)	5.5760(2)	4.4397(2)	70.50	*Pmnm*	23
		2.8544(2)	5.7020(2)	4.3420(2)	70.67		
Monoclinic (β=112.9^o)	1	5.63(1)	2.860(4)	5.77(1)	85.58	*C2/m*	36
Orthorhombic	1	4.77(1)	2.852(3)	6.31(2)	85.84	*Pmmn*	36

Table S4: Lattice parameter of the observed phases at room temperature.

Sample	Crystal system	Space group	*a* (Å)	*b* (Å)	*c* (Å)	Vol. (Å^3)
NC	Hexagonal	*P6$_3$/mmc*	2.8656(3)	2.8656(3)	11.1529(16)	79.312(16)
PC	Hexagonal	*P6$_3$/mmc*	2.8895(2)	2.8895(2)	11.1017(10)	80.273(12)
FC	Hexagonal	*P6$_3$/mmc*	2.8580(2)	2.8580(2)	11.1701(13)	79.015(15)
PD	Hexagonal	*P6$_3$/mmc*	2.8934(4)	2.8934(4)	11.1198(19)	80.622(23)
FD_R	Hexagonal	*P6$_3$/mmc*	2.9358(28)	2.9358(28)	10.9472(48)	81.71(10)
FD	Orthorhombic	*Cmcm*	2.8951(5)	5.4967(9)	10.7843(30)	171.61(8)
FD_R	Orthorhombic	*Cmcm*	2.9014(6)	5.4808(12)	10.8020(43)	171.78(10)
FD	Monoclinic (β=111.74(4)^o)	*C2/m*	5.794(15)	2.8593(11)	5.745(13)	88.409(49)
FD_R	Monoclinic (β=111.83(6)^o)	*C2/m*	5.8205(27)	2.8657(20)	5.774(25)	89.410(79)

Table S5: Statistical analysis determined from Rietveld-refinements. These are used for phase identification of the FD_R sample.

Combination	R_{wp} (%)
OOH	10.599
OHM	5.553
HOO	6.609
OHH	6.653
OOM	7.055
OMM	6.69
HHM	8.355
HMM	8.155
OOO	8.474
MMM	7.685
HHH	10.309

O-Orthorhombic, H-Hexagonal, M-Monoclinic

Table S6: Statistical analysis determined from Rietveld-refinements. These are used for phase identification of the FD sample.

Combination	R_{wp} (%)
HH	7.946
OO	7.398
OH	6.995
OM	5.111

O-Orthorhombic, H-Hexagonal, M-Monoclinic

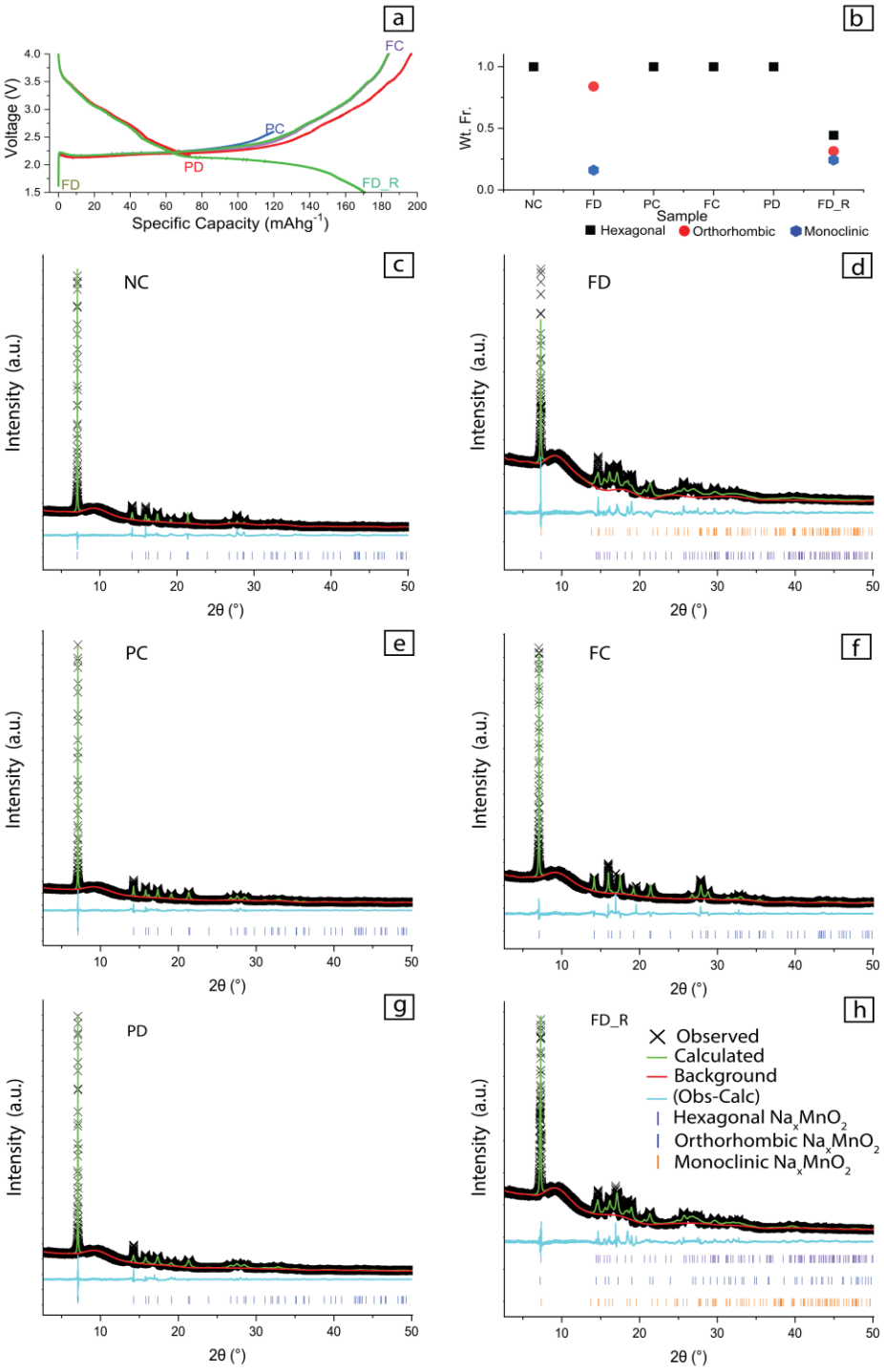

Figure S6. Evolution during electrochemical cycling, (a) charge-discharge curve showing points of extraction on the 2nd cycle (b) weight fraction as a function of the state of charge (c) – (h) Rietveld-refined fits of structural models to the XRD data (λ = 0.68729(1) Å) at the points of extraction shown in (a).

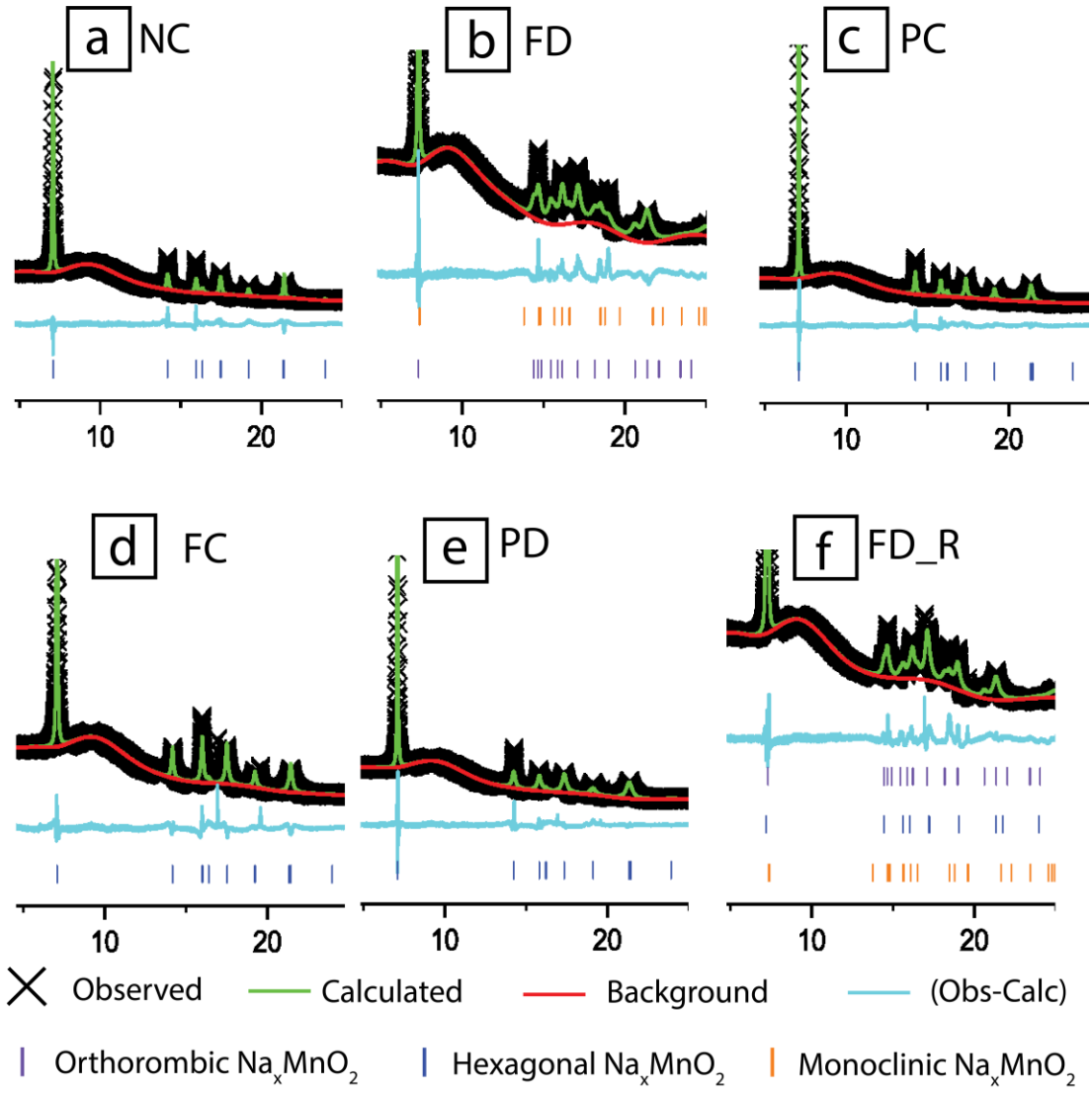

Figure S7. (a) – (f) Zoomed Rietveld refined fits of structural models to XRD data as a function of state of charge.

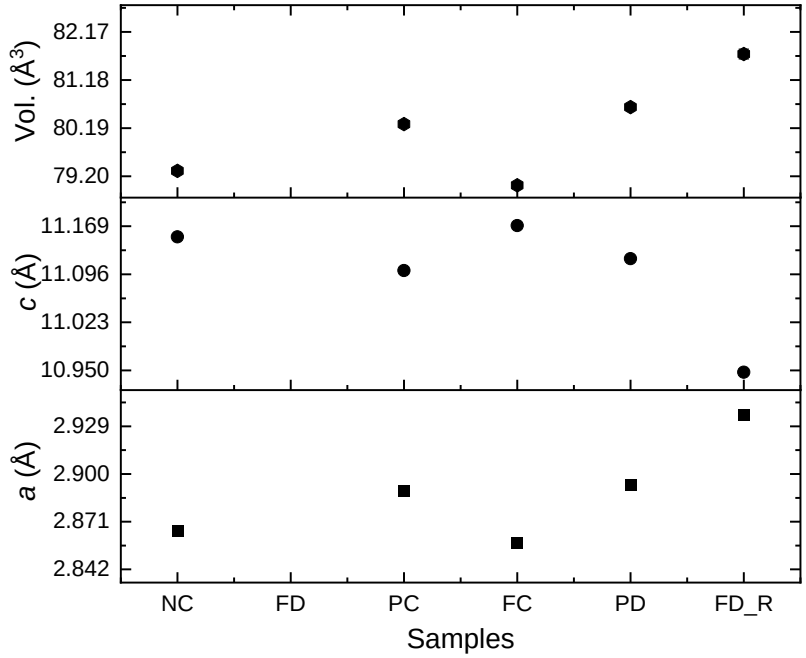

Figure S8: Electrochemical evolution of lattice parameters in the hexagonal $P6_3/mmc$ phase at room temperature.

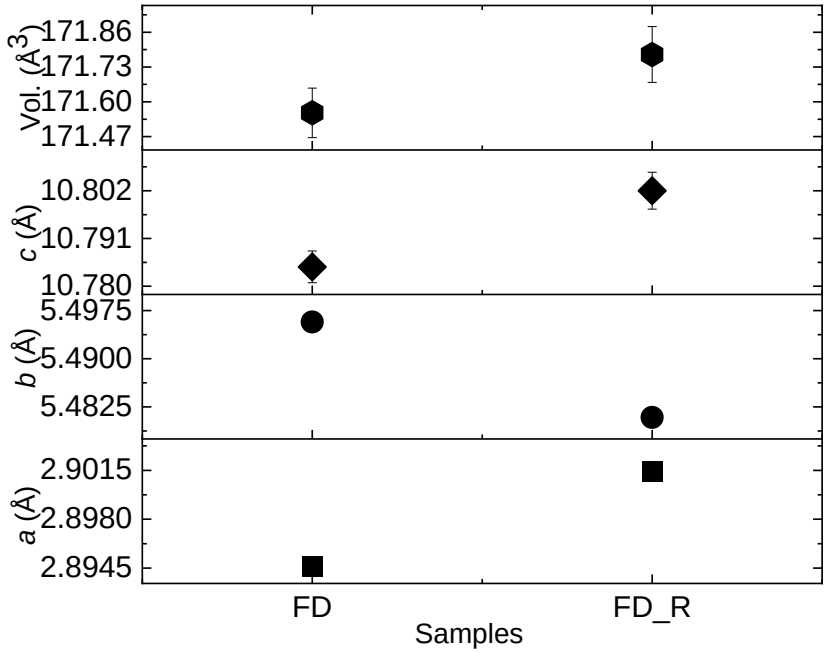

Figure S9: Electrochemical evolution of lattice parameters in the orthorhombic *Cmcm* phase at room temperature.

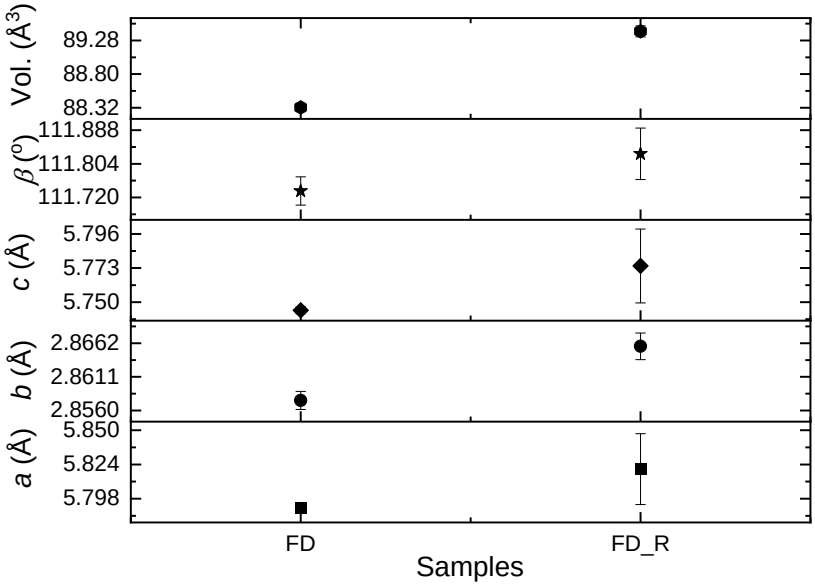

Figure S10: Electrochemical evolution of lattice parameters in the monoclinic *C*2/*m* phase at room temperature.

Table S7: Literature summary of *in situ* electrochemical studies on $Na_xMn_yB_zO_2$, where B is another transition metal and y+z = 1.

Initial Composition	Discharged/Charged	X value/voltage	Phases	Ref.
Orthorhombic Na_xMnO_2	Charging	0.2<x< 0.64	P'2-I	6
		x< 0.3	OP4	
	Discharging	x< 0.3	OP4	
		0.2<x< 0.6	P'2-I	
		x> 0.64	P'2-II	
Hexagonal Na_xMnO_2	Charging	Throughout the progress	P2	
	Discharging	Throughout the progress	P2	
		x>0.67	P'2-III	
Hexagonal Na_xMnO_2	Charging	x>0.55	P2+monoclinic (C2/c)[1]	29
		0.46<x<0.55	P2+monoclinic (C2/c)[2]	
		0.29<x<0.46	P2+monoclinic (C2/c)[3]	
		0.23<x<0.29	P2	
	Discharging	0.23<0.60	P2	
		0.60<x<0.74	P2+P'2	
		0.74<x<0.96	P'2	
Hexagonal $Na_{0.67}Al_{0.1}Mn_{0.9}O_2$	Charging	x>0.32	P2	
	Discharging	0.32<x<0.78	P2	
		0.78<x<0.98	P2+P'2	
Hexagonal $Na_{0.67}MnO_2$	Charging	0.1C up to 4 V	P2	24
	Discharging	0.1C 2.1-1.8 V	P2'	
		0.1C 1.5 V	P2+P2'	
$Na_{0.67}MnO_2$	1st charge	0.6-0.36	Hydrated, P2 and C2/c	39
		x<0.36	Hydrated, P2	
	1st discharge	x=0.99	P'2	
	2nd charge	x>0.67	P2, trace P'2	
		0.42>x>0.32	P2, and C2/c	
	2nd discharge	0.42<x<0.93	P2	
		x<0.93	P2, P'2	
Na_xMnO_2	Discharging	3 V, 15 mA.g^{-1}	P2 (1-4, 4 phases)	14
		2.5 V, 15 mA.g^{-1}	P2 (1-4, 4 phases)	
	Charging	2.9 V, 15 mA.g^{-1}	P1-P4	
		3.3 V, 15 mA.g^{-1}	P1-P5	
		3.6 V, 15 mA.g^{-1}	P1-P5	

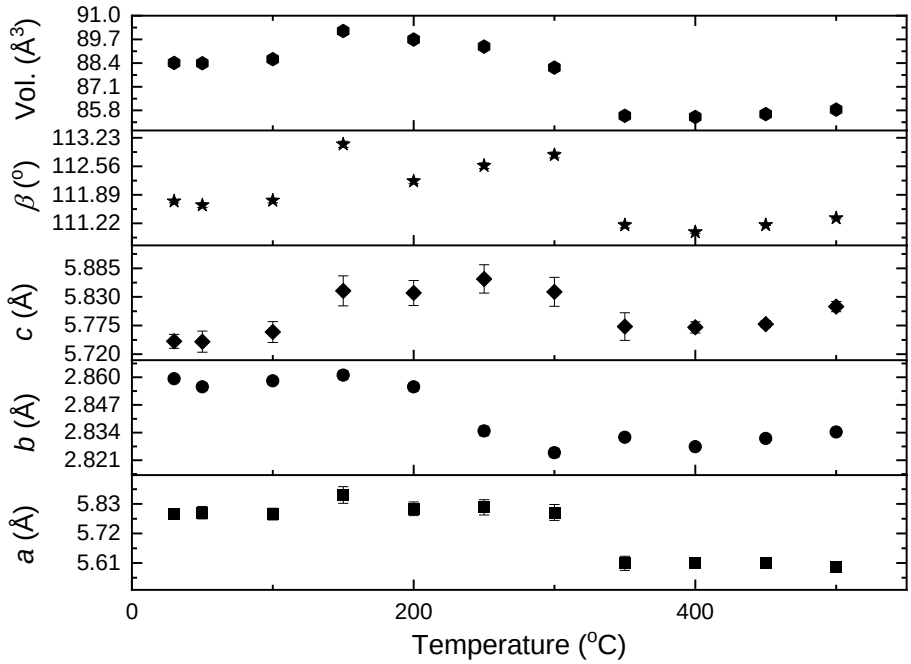

Figure S 11. Thermal evolution of the monoclinic phases in sample FD from room temperature to 550°C.

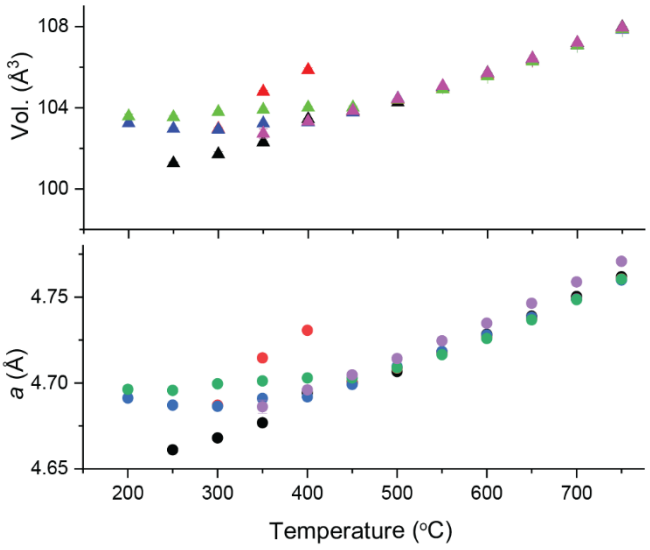

Figure S12. Lattice parameter and volume evolution of the NaF phase found between 200-750°C.

Table S8: Statistical analysis determined from Rietveld-refinements. These are used for phase identification. The first phase transition either to hexagonal or orthorhombic Na_xMnO_2 in each sample during the thermal evolution.

Sample	R_{wp} (%)	
	H to H	H to O/O to O
NC (300°C)	4.524	5.34
FD (150°C)	4.913	4.076
PC (350°C)	5.811	8.353
FC (300°C)	5.287	5.465
PD (300°C)	5.02	5.363

O-Orthorhombic, H-Hexagonal

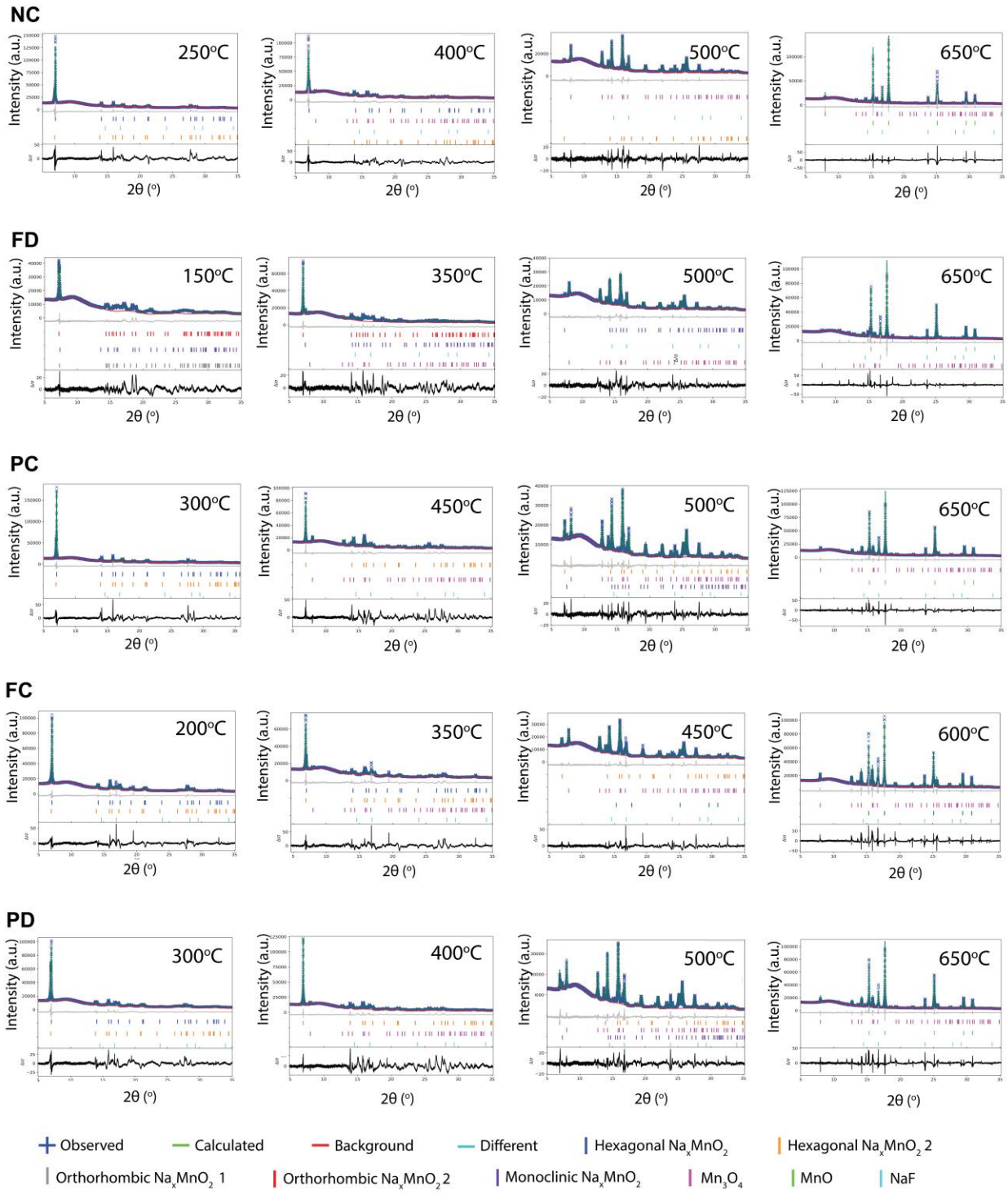

Figure S13: Selected Rietveld-refined fits for the thermal evolution of Samples NC to PD.

Table S9: Lattice parameter and volume for the thermal evolution of the original hexagonal phase.

Temp.	*a* (Å)				*c* (Å)				Volume (Å^3)			
(°C)	NC	PC	FC	PD	NC	PC	FC	PD	NC	PC	FC	PD
30	2.8656(3)	2.8895(2)	2.8580(2)	2.8934(4)	11.1529(16)	11.1017(10)	11.1701(13)	11.1198(19)	79.312(16)	80.273(12)	79.015(15)	80.622(23)
50	2.8660(3)	2.8898(2)	2.8584(2)	2.8933(4)	11.1591(16)	11.1063(10)	11.1759(13)	11.1259(19)	79.380(16)	80.324(12)	79.081(15)	80.660(22)
100	2.8673(3)	2.8898(2)	2.8599(2)	2.8903(4)	11.1746(18)	11.1237(10)	11.1907(13)	11.1488(19)	79.565(18)	80.449(12)	79.266(15)	80.657(22)
150	2.8686(3)	2.8883(2)	2.8622(2)	2.8862(4)	11.1894(18)	11.1471(10)	11.2052(13)	11.1798(20)	79.742(17)	80.532(11)	79.498(15)	80.653(23)
200	2.8698(3)	2.8853(2)	2.8653(2)	2.8842(4)	11.2085(19)	11.1785(10)	11.2172(14)	11.219(21)	79.944(19)	80.594(12)	79.755(16)	80.824(24)
250	2.8672(3)	2.8832(3)	2.8655(3)	2.8784(5)	11.2081(19)	11.2112(14)	11.2286(20)	11.2441(25)	79.793(19)	80.712(16)	79.844(23)	80.681(29)
300	2.8627(7)	2.8792(5)	2.8609(9)	2.8741(7)	11.2087(27)	11.2237(20)	11.2479(41)	11.2588(31)	79.549(34)	80.577(26)	79.725(50)	80.545(39)
350	2.8580(47)	2.8777(16)	2.8532(23)	2.8680(20)	11.234(35)	11.2340(33)	11.2713(40)	11.2817(32)	79.469(161)	80.569(65)	79.463(87)	80.364(72)
400	2.8308(25)	2.8624(12)		11.2607(33)	11.2517(44)			78.146(88)	79.840(406)			

Table S10: Lattice parameter and volume for the thermal evolution of the secondary hexagonal phase.

Temp.	*a* (Å)				*c* (Å)				Volume (Å^3)			
(°C)	NC	PC	FC	PD	NC	PC	FC	PD	NC	PC	FC	PD
200			2.8851(25)				11.4305(15)				82.397(85)	
250	2.8746(21)		2.9097(8)	2.8886(27)	11.4020(7)		11.4362(7)	11.3951(7)	81.598(72)		83.848(28)	82.343(93)
300	2.8779(86)	2.8854(11)	2.9004(6)	2.9030(9)	11.4398(24)	11.3591(5)	11.4325(7)	11.4174(5)	82.056(293)	81.901(38)	83.288(21)	83.328(32)
350	2.8895(9)	2.8897(7)	2.8974(5)	2.9024(6)	11.4034(4)	11.3773(3)	11.4283(10)	11.4167(6)	82.454(32)	82.276(25)	83.087(19)	83.287(20)
400	2.8984(4)	2.9007(10)	2.8971(5)	2.895(7)	11.4243(9)	11.3733(8)	11.4119(6)	11.3659(15)	83.113(15)	82.876(34)	82.952(18)	82.496(27)
450	2.8992(6)	2.8974(5)	2.8945(21)	2.8957(18)	11.3782(4)	11.3211(7)	11.3541(13)	11.3261(18)	82.824(22)	82.309(16)	82.379(71)	82.244(63)
500	2.9026(33)	2.9056(5)		2.8951(11)	11.3066(19)	11.2554(8)		11.359(7)	82.498(112)	82.291(18)		82.449(37)

Table S11: Lattice parameter and volume for the thermal evolution of both orthorhombic phases in the FD sample.

Temp. (°C)	*a* (Å)		*b* (Å)		*c* (Å)		Volume (Å^3)	
	FD_1	FD_2	FD_1	FD_2	FD_1	FD_2	FD_1	FD_2
30	2.8951(5)		5.4967(9)		10.7843(30)		171.61(8)	
50	2.8949(6)		5.4958(13)		10.7873(41)		171.62(10)	
100	2.8939(6)		5.4930(11)		10.8055(38)		171.77(9)	
150	2.8752(29)	2.9027(27)	5.4890(28)	5.3203(22)	10.8480(44)	11.0017(45)	171.21(19)	169.90(16)
200	2.8762(44)	2.8856(17)	5.5215(39)	5.2712(17)	10.9185(44)	11.0619(43)	173.39(28)	168.78(12)
250	2.8362(66)	2.8780(17)	5.5913(57)	5.2876(17)	10.9670(40)	11.1390(39)	173.92(46)	168.99(12)
300		2.8578(8)		5.2796(17)		11.2118(50)		169.16(11)
350		2.8512(7)		5.3249(16)		11.2416(50)		170.67(12)
400		2.8554(6)		5.3615(13)		11.2018(23)		171.49(7)

Table S12: Lattice parameter and volume for the thermal evolution of the tetragonal Mn_3O_4 phase.

Temp.	*a* (Å)					*c* (Å)					Volume (Å^3)				
(ºC)	FD	NC	PC	FC	PD	FD	NC	PC	FC	PD	FD	NC	PC	FC	PD
350	5.7784(27)	5.7587(24)	5.7724(12)	5.7884(17)	9.4997(44)	9.6140(65)	9.4736(25)	9.4763(35)	317.20(32)	318.83(27)	315.66(18)	317.51(22)			
400	5.7762(7)	5.7804(7)	5.7846(19)	5.7769(4)	5.7856(11)	9.4971(12)	9.4963(17)	9.4933(37)	9.4845(8)	9.4814(21)	316.86(10)	317.30(11)	317.66(26)	316.52(6)	317.37(15)
450	5.7772(4)	5.7789(3)	5.7806(13)	5.7781(3)	5.7804(13)	9.5119(8)	9.5051(6)	9.5039(23)	9.4959(7)	9.4975(25)	317.47(6)	317.43(5)	317.57(19)	317.03(5)	317.34(21)
500	5.7818(1)	5.7801(2)	5.7794(3)	5.7817(1)	5.7800(3)	9.5182(3)	9.5176(4)	9.5187(5)	9.5182(3)	9.5174(5)	318.18(1)	317.98(3)	317.94(4)	318.18(1)	317.96(4)
550	5.7806(3)	5.7813(2)	5.7800(2)	5.7823(1)	5.7804(2)	9.5290(6)	9.5287(3)	9.5296(4)	9.5277(3)	9.5280(4)	318.41(5)	318.48(3)	318.37(3)	318.55(1)	318.35(3)
600	5.7823(2)	5.7834(2)	5.7815(2)	5.7837(1)	5.7819(2)	9.5358(5)	9.5360(3)	9.5369(3)	9.5360(3)	9.5347(4)	318.83(3)	318.95(3)	318.78(3)	318.99(1)	318.99(1)
650	5.7842(3)	5.7845(2)	5.7834(2)	5.7842(5)	5.7838(2)	9.5411(7)	9.5417(4)	9.5427(4)	9.5371(14)	9.5409(4)	319.21(3)	319.27(3)	319.18(2)	319.08(6)	319.08(6)

Table S13: Lattice parameter for the thermal evolution of the cubic MnO phase.

Temp.	*a* (Å)					Volume (Å^3)				
(ºC)	FD	NC	PC	FC	PD	FD	NC	PC	FC	PD
550	4.4737(3)	4.4744(3)	4.4733(2)	4.4730(1)	4.4731(5)	89.537(16)	89.577(19)	89.515(13)	89.495(8)	89.500(28)
600	4.4768(1)	4.4771(1)	4.4764(1)	4.4765(0)	4.4757(1)	89.726(8)	89.740(8)	89.701(7)	89.704(2)	89.660(8)
650	4.4803(1)	4.4803(1)	4.4797(1)	4.4800(0)	4.4792(1)	89.932(4)	89.936(5)	89.900(5)	89.914(1)	89.865(5)
700	4.4836(1)	4.4839(1)	4.4832(1)	4.4830(0)	4.4828(1)	90.135(4)	90.149(6)	90.108(3)	90.094(1)	90.082(4)
750	4.4518(1)	4.4547(1)	4.4542(0)	4.4540(0)	4.4523(0)	88.226(4)	88.402(4)	88.369(2)	88.361(1)	90.288(4)
200	4.4547(1)	4.4542(0)	4.4540(0)	4.4523(0)	88.226(4)	88.402(4)	88.369(2)	88.361(1)	88.259(2)	88.260(4)
30	4.4460(1)	4.4454(0)	4.4449(0)	4.4429(0)	87.675(5)	87.885(4)	87.850(2)	87.821(1)	87.701(3)	87.701(5)

Table S14: Lattice parameter and volume for the thermal evolution of the monoclinic phase in the FD sample.

Temp. (°C)	*a* (Å)	*b* (Å)	*c* (Å)	β(°)	Volume(Å^3)
30	5.794(15)	2.8593(11)	5.745(13)	111.736(35)	88.409(49)
50	5.798(23)	2.8555(17)	5.744(20)	111.648(55)	88.387(70)
100	5.792(22)	2.8583(16)	5.763(20)	111.755(53)	88.610(66)
150	5.864(31)	2.8610(21)	5.842(28)	113.077(73)	90.156(95)
200	5.812(26)	2.8555(19)	5.838(24)	112.211(61)	89.691(83)
250	5.817(29)	2.8348(22)	5.865(27)	112.574(68)	89.302(82)
300	5.798(29)	2.8245(21)	5.840(28)	112.828(68)	88.148(85)
350	5.609(26)	2.8318(16)	5.773(27)	111.178(68)	85.505(74)
400	5.6090(10)	2.8273(7)	5.772(11)	111.014(27)	85.439(33)
450	5.6115(61)	2.8313(4)	5.778(6)	111.180(16)	85.594(22)
500	5.5958(90)	2.8343(6)	5.811(9)	111.344(24)	85.847(25)

Table S15: Lattice parameter and volume for the thermal evolution of the NaF phase.

Temp.(°C)	*a* (Å)					Volume (Å^3)				
	FD	NC	PC	FC	PD	FD	NC	PC	FC	PD
200				4.6913(8)	4.6963(16)				103.24(5)	103.58(11)
250		4.6611(10)		4.6871(7)	4.6957(13)		101.27(7)		102.97(5)	103.54(8)
300		4.668(17)	4.687(12)	4.6864(6)	4.6995(10)		101.72(11)	102.97(8)	102.93(4)	103.79(6)
350	4.6834(35)	4.6769(8)	4.7146(10)	4.6911(5)	4.7012(7)	102.73(23)	102.3(5)	104.79(7)	103.23(3)	103.9(5)
400	4.6925(9)	4.6943(4)	4.7307(14)	4.6919(3)	4.703(7)	103.33(6)	103.44(3)	105.87(9)	103.29(2)	104.02(4)
450	4.7005(4)	4.7006(2)	4.7000(5)	4.6991(2)	4.703(10)	103.86(2)	103.86(1)	103.82(3)	103.77(2)	104.02(7)
500	4.7093(2)	4.7067(1)	4.7086(1)	4.7096(1)	4.7089(1)	104.44(1)	104.27(0)	104.40(01)	104.46(1)	104.41(1)
550	4.7188(1)	4.7181(0)	4.7176(1)	4.7183(1)	4.7165(1)	105.08(1)	105.03(0)	104.99(1)	105.04(1)	104.92(1)
600	4.7283(1)	4.7284(1)	4.7271(1)	4.7280(1)	4.7259(1)	105.71(1)	105.71(0)	105.63(0)	105.69(0)	105.55(1)
650	4.739(1)	4.7389(1)	4.7377(1)	4.7383(0)	4.7368(1)	106.43(0)	106.42(0)	106.34(0)	106.38(0)	106.28(0)
700	4.7505(1)	4.7504(1)	4.749()	4.7488(0)	4.7485(1)	107.2(0)	107.20(0)	107.10(0)	107.09(0)	107.07(0)
750	4.7616(1)	4.7619(1)	4.7606()	4.7600(0)	4.7605(1)	107.96(0)	107.98(0)	107.89(0)	107.85(0)	107.88(0)
200	4.6615(1)	4.6618(1)	4.6614(0)	4.6615(0)	4.6621(1)	101.29(1)	101.31(1)	101.29(0)	101.33(0)	4.6615(1)
30	4.6374(1)	4.6379(1)	4.6368(1)	4.6363(0)	4.6377(1)	99.726(1)	99.764(1)	99.66(0)	99.75(0)	4.6374(1)

REFERENCES

[45] J. Akimoto, H. Hayakawa, N. Kijima, J. Awaka, F. Funabiki, Solid State Phenomena, 2011, Vol. 170, pp 198–202. https://doi.org/10.4028/www.scientific.net/SSP.170.198

[46] C. Fu, J. Wang, Y. Li, G. Liu, T. Deng, J Alloys Compd, 2022, 918. https://doi.org/10.1016/j.jallcom.2022.165569

[47] S. P. Vanam, B. Senthilkumar, P. Amonpattaratkit, P. Barpanda, Inorg Chem, 2022, 61 (9), 3959–3969. https://doi.org/10.1021/acs.inorgchem.1c03609

[48] R. Hoppe, G. Brachtel, M. Jansen, ZAAC - Journal of Inorganic and General Chemistry, 1975, 417 (1), 1–10. https://doi.org/10.1002/zaac.19754170102

[49] M. Jansen, R. Hoppe, ZAAC - Journal of Inorganic and General Chemistry, 1973, 399 (2), 163–169. https://doi.org/10.1002/zaac.19733990204